Effect of V/III molar ratio on the structural and optical properties of InN epilayers grown by HPCVD

Ramazan Atalay*[a], Max Büegler[a,b], Sampath Gamage[a], M. K. Indika Senevirathna[a], Bahadır Küçükgök[c], Andrew G. Melton[c], Axel Hoffmann[b], A. G. Unil Perera[a], Ian T. Ferguson[c], and Nikolaus Dietz[a]

[a]Department of Physics and Astronomy, Georgia State University, Atlanta, GA 30303

[b]Institut für Festkörperphysik, Technische Universität Berlin, Berlin, Germany

[c]Dept. of Elect. & Comp. Engineering, University of North Carolina Charlotte, Charlotte, NC 28223

ABSTRACT

The dependency of the structural and optoelectronic properties of InN thin films grown by high-pressure chemical vapor deposition technique on the group V/III molar precursor ratio has been studied. X-ray diffraction, Raman spectroscopy, and IR reflectance spectroscopy have been utilized to study local- and long-range structural ordering as well as optoelectronic properties of the InN epilayers grown on crystalline sapphire substrates. The investigated InN epilayers were grown with group V/III molar precursor ratio varying from 900 to 3600, while all other growth parameters were kept constant. For a group V/III precursor ratio of 2400, the full width-half maximum of the Raman E_2(high) mode and XRD (0002) Bragg reflex exhibit minimums of 7.53 cm^{-1} and 210 arcsec, respectively, with maximized grain size and reduced in-plane strain effect. FTIR data analysis reveals a growth rate of 120 nm/hr, a carrier mobility of 1020 $cm^2V^{-1}s^{-1}$, and a free carrier concentration of 1.7×10^{18} cm^{-3} for a V/III ratio of 2400. The Raman analysis indicate that non-polar E_2(high) mode position remains unaffected from a changing V/III ratio; whereas, polar A_1(LO) mode position significantly changes with changing V/III ratio. Optical analysis also suggests that LO-phonon correlates with free carrier concentration (n_e) and TO-phonon correlates with free carrier mobility (μ) in the InN epilayers.

Keywords: Indium nitride (InN), V/III molar ratio, X-ray diffraction, Raman spectroscopy, Infrared (IR) reflectance spectroscopy, HPCVD.

*atalay@phy-astr.gsu.edu; phone (404) 413 6033; fax 404 413-6025; http://www.phy-astr.gsu.edu/dietz/.

1. INTRODUCTION

Indium nitride (InN) has received a renewed attention due to the recent downward revision of its band gap from 1.8 eV to below 0.7 eV as well as for its superior electron transport properties.[1,2] InN has one of the smallest effective mass of all the group III-nitride semiconductors, which leads to its predicted high-electron mobility[3] of ~ 4400 $cm^2V^{-1}s^{-1}$, a high saturation velocity,[2] and large drift velocity at room temperature. Possessing a direct bandgap of 0.7 eV,[2] InN is also a potential material candidate for IR emission or sensing applications.[4] In addition to its potential use in high-frequency/high-power electronic devices[2-4] and infrared optoelectronics,[5] ternary or quaternary alloying of In(AlGa)N material allows a tailoring of the bandgap from near-infrared to the ultraviolet (6.2 eV) spectral region. Therefore, the development and integration of InN and In-rich ternary alloys (e.g. $In_{1-x}Ga_xN$ and $In_{1-x}Al_xN$) opens new avenues for the fabrication of THz emitters or detectors,[6] chemical sensor applications,[7] and high-efficient energy conversion devices, such as solid state lightning,[8] multi-tandem photovoltaics,[8] and monolithically integrated LED displays.[9]

At present, the growth of high-quality InN material by conventional deposition techniques is limited due to low dissociation temperature of InN (~ 600 °C) and large differences in the partial pressures of the group III-V constituents. Thus, for the stabilization of InN by off-equilibrium growth techniques such as plasma-assisted molecular beam epitaxy (MBE)[10] have been successfully applied in the growth of InN epilayers and InGaN alloys at relatively low temperatures in the range of 460-500 °C. However, the low growth rates in MBE limits its application and integration with present industrial processing technology. Low-pressure metal organic chemical vapor deposition (MOCVD),[11] which is presently to dominant industrial processing tool for GaN and gallium-rich GaAlInN alloys has a very limited process

Twelfth International Conference on Solid State Lighting and Fourth International Conference on White LEDs and Solid State Lighting, edited by Matthew H. Kane, Christian Wetzel, Jian-Jang Huang, Ian T. Ferguson, Proc. of SPIE Vol. 8484, 84840X · © 2012 SPIE · CCC code: 0277-786/12/$18 · doi: 10.1117/12.930199

parameter space, limiting its ability to suppress dissociation of InN epilayers. Hacker *et al.*[12] have intensively studied comprehensive cracking processes of ammonia at various pressures and temperatures. Ammonia is a very stable molecule and its cracking efficiency is quite low at low growth temperatures; therefore, in order to achieve epitaxial growth of InN, very high ammonia partial pressure, i.e., V/III ratio, is required. Johnson *et al*.[13] have reported the use of pulsed MOCVD, where ammonia is constantly flowing while the TMI precursor is periodically injected into the reaction zone to overcome stabilization problem.

In this contribution, the growth InN epilayer is explored at super-atmospheric reactor pressure in order to suppress the surface dissociation of InN, which can be avoided at elevated ambient-nitrogen (N_2) pressures. Superatmospheric MOCVD, denoted here as high-pressure chemical vapor deposition (HPCVD), provides processing parameter addition needed to narrow the processing gap between the binaries InN and GaN.[14-16]

In this paper, the dependency of the structural and optoelectronic properties of InN epilayers on the group V/III molar precursor ratio were investigated. The structural and optoelectronic properties were analyzed by X-ray diffraction, Raman spectroscopy, and Fourier transform infrared reflectance (FTIR) spectroscopy.

2. EXPERIMENTAL DETAILS

InN epilayers studied in this contribution were grown on sapphire (0001) substrate by HPCVD with a horizontal flow channel reactor.[14] Trimethylindium (TMI) and ammonia (NH_3) precursors, utilized as indium and nitrogen sources, respectively, transported to the reaction zone using nitrogen as a carrier gas. A unique pulsed precursor-injection mechanism was employed, which is a precise sequential control of the precursors pulse width, pulse separations, and total cycle duration as added process parameters to adjust gas phase and surface reactions. Since the details of the HPCVD reactor system have been published previously,[14-16] only key parameters are restated in here. The epitaxial deposition process was carried out at group V/III molar precursor ratio, varying from 900 to 3600. The TMI and NH_3 pulse width were kept constant at 0.8 and 1.643 s with a TMI flow rate of 22.21 μmol/min and an ammonia flow of 1200 sscm. The reactor pressure was set to 8 bar with a total carrier gas flow of 12 standard liter per minute (slm).

The structural and optoelectronic properties of the InN samples have been analyzed by utilizing X-ray diffraction (XRD), Raman spectroscopy, and FTIR spectroscopy. XRD measurements were carried out utilizing a Philips X'Pert PRO MPD X-ray diffractometer equipped with monochromatic Cu-$K_{\alpha 1}$ (λ = 1.540598 Å) source. A triple axis configuration was used for the 2θ-ω scans normal to *c*-plane of a sample. The 2θ-ω triple axis scans were analyzed by PseudoVoigt curve fitting algorithm to determine position and full-width at half maximum (FWHM) of the Bragg reflexes. The *c*-axis value (lattice parameter), crystallite size, and in-plane strain along the epilayers were calculated. The broadening of crystallite size was calculated by Scherrer formula given by the following relation:[17]

$$D_{2\theta} = \frac{K \cdot \lambda}{\beta_{2\theta} \cdot \sin\theta}, \tag{1}$$

where the constant K (the Scherrer constant) is the shape factor taken to be 0.94 (assuming a FWHM of spherical crystal with cubic symmetry), $\beta_{2\theta}$ is the linewidth of Bragg reflex (in radians), and 2θ is the Bragg angle. The analysis of the crystallite size from XRD Bragg reflex allows estimating the domain size as well as extended defects. The systematic shifts of atoms from their ideal position leads to an in-plane strain component that contributes to the line broadening.[19] The strain component in the epitaxial layer can be determined by the in-plane strain relation:

$$E_{2\theta} = \frac{\beta_{2\theta}}{4 \cdot \tan\theta}. \tag{2}$$

Raman spectroscopy was applied to analyze the bonding and local ordering of the InN epilayers. The custom-configured Raman spectrometer uses a liquid N_2-cooled multichannel charge-coupled (CCD) camera and a McPherson double subtractive monochromator in combination with a single 2m monochromator system to record the inelastic Raman scattering. The Raman measurements were carried out in back scattering geometry along the (0001) crystalline plane using excitation energy of 2.33 eV at room temperature. For FTIR spectroscopy, a Perkin-Elmer 2000 system was utilized. The FTIR experiments were carried out at room temperature in the energy range of 0.04965 to 0.8068 eV in near-normal incidence (~8°) geometry. The free carrier concentration and carrier mobility of InN epilayers were

obtained by fitting the experimental FTIR spectra to theoretical model spectrum using multilayer stack theory and the Lorentz-Drude models.[18]

3. RESULTS AND DISCUSSION

Figure 1a depicts the results obtained from the XRD analysis of the InN epilayers. The left side in Fig. 1a shows the FWHM values of the InN (0002) Bragg reflex with the calculated *c*-axis parameter displayed on the (right scale) as a function of V/III precursor ratio. The FWHM values increase with increased V/III ratio from 900 to 1800 and decrease afterwards for V/III precursor of 2400 with a FWHM minimum of 210 arcsec. As the group V/III molar precursor ratio is further increased from 2400 to 3600, the FWHM values increase again. Both the FWHM values for the InN (0002) Bragg reflex as well as the Bragg reflex center position follow the same trend, which might be due to relaxation of the grains or due to relaxation of stacking layers. For the group V/III precursor ratio of 2400, the FWHM of the (0002) Bragg reflex reaches a minimum and calculated *c*-axis lattice parameter approaches the theoretically relaxed value of 5.712 nm.

The calculated grain size and in-plane strain values (Eqn. 1 and 2) are presented in Fig. 1b. as a function of the V/III molar precursor ratio. As depicted in Fig. 1b, the crystallite size along the in-plane direction decreases for V/III ratio up to 1800 and it increases afterwards with maximum at 2400 and decreases again for higher V/III ratio. The computed strain effect as a function of group V/III molar precursor ratio shows an inverse behavior with the grain size. The structural properties extracted from XRD analysis for the InN epilayers grown under various group V/III molar ratio are summarized in Table 1. The correlation of these data with the local crystalline ordering (Raman analysis) and phonon characteristic (FTIR analysis) will be followed below.

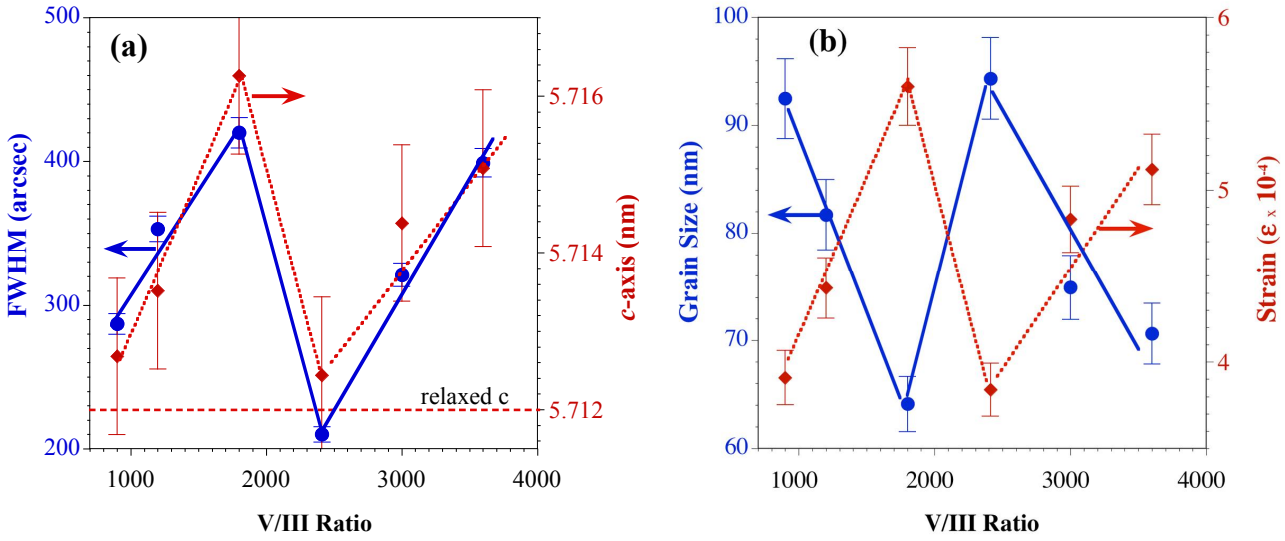

Figure 1. Group V/III molar precursor ratio dependence of the X-ray diffraction (2θ-ω) TrAx analyses for HPCVD grown InN epilayers. (a) FWHM (left scale) and *c*-axis length (right scale) as a function of V/III ratio. (b) Grain size (left scale) and in-plane strain (right scale) as a function of V/III ratio.

The wurtzite (hexagonal) InN crystal structure belongs to a space group of $P6_3mc$ with two formula units per unit cell. The Raman-active zone-center optical phonons predicted by the group theory are $A_1+2B_1+E_1+2E_2$.[19] Phonons of A_1 and E_1 symmetries are polar and exhibit a wave number splitting for transverse optical (TO) and longitudinal optical (LO) branches. The non-polar phonon mode with E_2 symmetry has a two-fold energy and vibrational degeneracy. The E_2(high) and E_2(low) phonons are associated with nitrogen and indium sublattice vibrations, respectively. The representative E_2(high) spectra for various group V/III precursor ratios are shown in Fig. 2a. The E_2(high) phonon mode is centered at 488.5 cm^{-1}, which is in good agreement with reported literature values.[19]

The FWHM values for the E_2(high) and its center peak positions are depicted in Fig. 2b. Peak position values reveal a stagnant E_2(high) vibrational mode position as function of the group V/III precursor ratio. However, the FWHM values of the E_2(high) mode decrease with increasing V/III precursor ratio, showing a local optimum at 2400 and an increase of FWHM values as V/III ratio is further increases. The results indicate that the V/III ratio of 2400 is a local optimum for the local/microscopic ordering. Although the linewidth of E_2(high) mode evidently changes with varying V/III ratio, the peak center remains stagnant. This could indicate that microscopic ordering in the epilayer has a neglectable influence on the overall crystallinity of the InN epilayer, i.e., microscopically relaxed material.

Table 1. Summary of the structural properties obtained from X-ray diffraction (2θ-ω) analyses, linewidth, interplanar spacing, grain size, and in-plane strain of the HPCVD grown InN thin films of different group V/III precursor ratio.

V/III Ratio	Angle 2θ (°)	$\beta_{2\theta}$ (arcsec)	c-axis Å	Grain size (nm)	Strain (ε 10^{-4})
900	31.32	287	5.713	92.5	3.90
1200	31.33	353	5.714	81.7	4.41
1800	31.31	420	5.716	64.1	5.60
2411	31.33	210	5.712	94.4	3.83
3000	31.32	321	5.714	74.6	4.82
3600	31.32	399	5.715	70.6	5.11

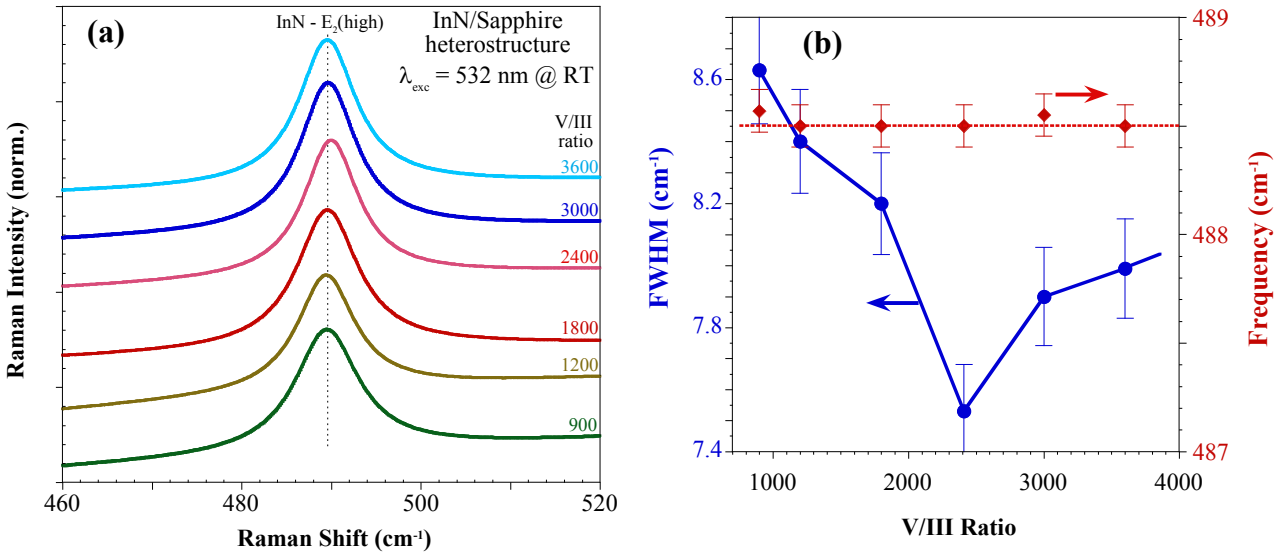

Figure 2. Group V/III molar precursor ratio dependence of the E_2(high) phonon mode. (a) Measured Raman spectra for group V/III molar precursor ratio between 900 and 3600 along the (0001) plane. (b) FWHM (blue squares, left axis) and frequency (red circles, right axis) as a function of group V/III molar precursor ratio.

The representative Raman spectra in the vicinity of the A_1(LO) phonon mode as a function of the group V/III precursor ratio are shown in Fig. 3a. The center of the A_1(LO) mode peak is observed in the proximity of 591 cm^{-1}, which agrees well with literature values.[19] As depicted Fig. 3a, a distinct broadening and frequency shifting of the A_1(LO) mode can be observed with change of the group V/III precursor ratio. The relevant data, FWHM and peak center frequency are given in Fig. 3b. With increasing V/III precursor ratio from 900 to 2400, the FWHM values of the A_1(LO) mode decrease to a minimum value of 16.4 cm^{-1}. For higher V/III precursor ratio, the FWHM values increase again. The broadening of A_1(LO) mode can arise from some defects, such as nitrogen vacancies, indium interstitials, and from their complexes.[20] Although the assignment of the LO-phonon-plasmon coupled mode in InN material is under discussion,[21,22] a broadening of the A_1 mode due to an plasmonic influence contribution. For the V/III ratio of 2400, the frequency of the A_1(LO) mode shows a local minimum of 590.5 cm^{-1}. Results from the Gaussian-fitting analysis of the vibrational

A_1(LO) mode indicate that asymmetric broadening is affects more to the lower frequency side for smaller V/III ratios of 900 and 1200. In order to understand and correlate the asymmetric broadening mechanism of the A_1(LO) mode, the phonon response in the infrared region will be followed by FTIR spectroscopy.

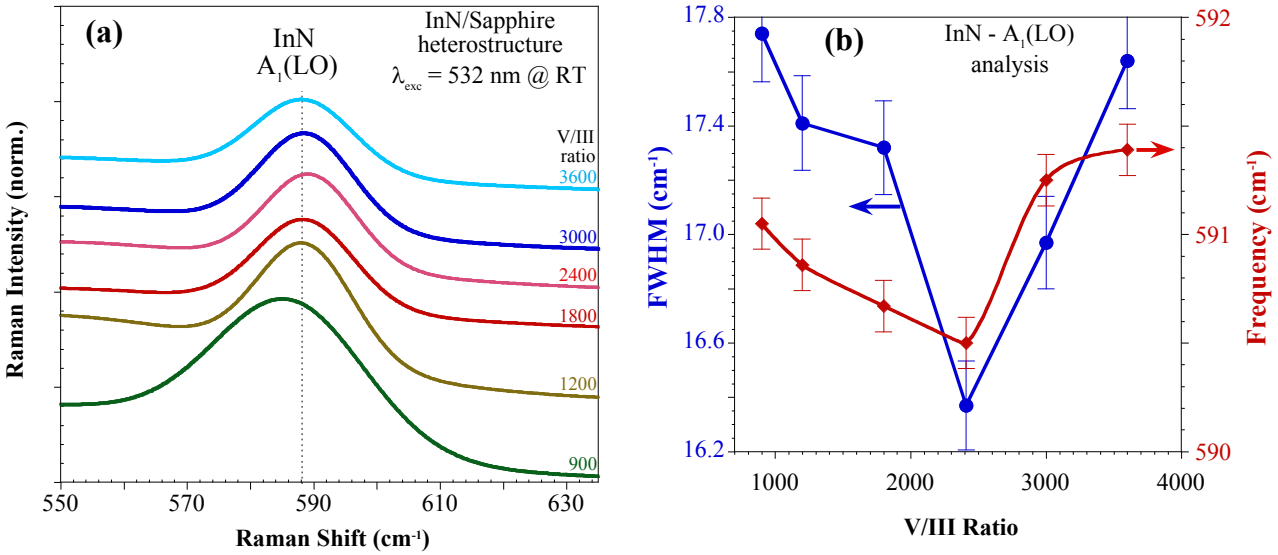

Figure 3. Group V/III molar precursor ratio dependence of the A_1(LO) phonon mode. (a) Measured Raman spectra for group V/III molar precursor ratio between 900 and 3600 along the (0001) plane. (b) FWHM (blue squares, left axis) and frequency (red circles, right axis) as a function of group V/III molar precursor ratio.

FTIR spectra acquired in normal-incidence configuration in the spectral range between 400 cm^{-1} and 8000 cm^{-1} where analyzed using a multilayer stack model[18]. The fitting results provide information on the layer structure, and were used to determine the layer thickness, growth rate broadening constant, electron mobility, LO and TO phonon frequencies, as well as free carrier concentration of the InN epilayers, as summarized in Table 2. The InN dielectric function, used in these calculations, is based on the Drude-Lorentz model, which couples the contributions of plasma oscillations and phonons by classical Drude model and by Lorentzian type oscillator model, respectively.[18]

Figure 4a shows the estimated layer thicknesses (left axis) and free carrier concentrations (right axis) of the InN epilayers as a function of the group V/III precursor ratio. The thinner InN layer thicknesses for the V/III ratios of 900 and 1200 may explain the observed asymmetric broadening of the A_1(LO) mode to the lower frequency side in the Raman spectra discussed above. It is crucial to express a profound principle in the phonon dynamic that wave vectors in the range of 500-600 cm^{-1} and 600-700 cm^{-1} may result in anharmonic phonon decay in InN.[23] Even though there is not universally accepted layer thickness for which the harmonic decay channel in epilayer is considered to be optically relaxed, the experimental data analyzed in here indicate that the InN epilayer thickness should be larger than 100 nm. The data in Fig. 4 show that the growth rates and with it the total layer thicknesses increase significantly with increasing V/III molar precursor ratio from 900 to 2400, with leveling in slight decrease in the growth rate for higher V/III ratios. As depicted in Fig. 4a, the FTIR data analysis also revealed the that free carrier concentration drops with increasing layer thickness, with the lowest free carrier concentration of 1.8×10^{18} cm^{-3} obtained for a V/III ratio of 2400. The here obtained values for the free carrier concentration are still high compared to recent reported free carrier concentration of 5.6×10^{17} cm^{-3} for InN epilayers grown on GaN by plasma-assisted molecular beam epitaxy (PAMBE).[24]

The carrier mobility together with the InN epilayer thickness as function of group V/III molar precursor ratio is shown in Fig. 4b. Even though the free carrier mobility oscillates with increasing V/III ratio, both layer thickness and free carrier mobility exhibit a maximum of 360 nm (growth rate of 2 nm/min) and 1020 $cm^2V^{-1}s^{-1}$ respectively, for a V/III precursor ratio of 2400. Lin *et al.*[25] reported the InN epilayer growth on GaN/sapphire template by MOCVD with a V/III ratio of 18000, a carrier mobility of 1300 $cm^2V^{-1}s^{-1}$ and free carrier concentration of 4.6×10^{18} cm^{-3}.

As shown in Figs. 4a and 4b, the correlation of InN epilayer thickness with free carrier concentration, and free electron mobility is nonlinear, as growth surface topographic evolution and the influence of extended defects are not

considered. However, the increase of layer thickness positively influences the free electron mobility and inversely effects the free carrier concentration with increasing V/III ratio, as expected from the theory.[24,25] For V/III precursor ratio higher than 2500, access NH^*, related precursor fragments may alter the growth surface chemistry and the incorporation of impurity and formation of extended defects in the InN epilayers.[20]

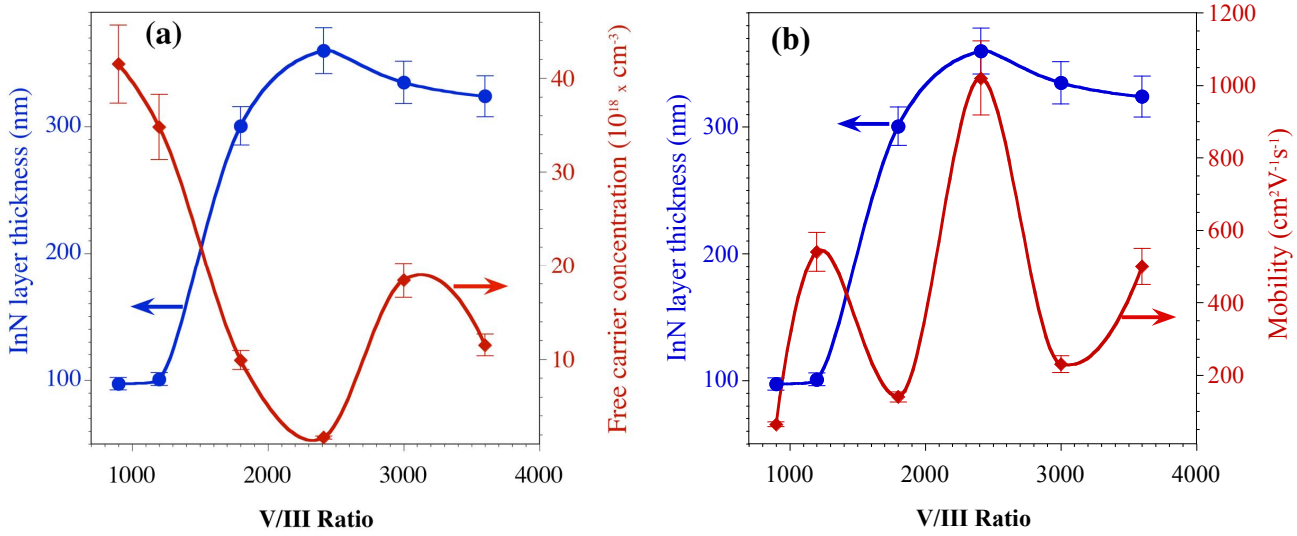

Figure 4. Group V/III molar precursor ratio dependence of the IR reflectance spectroscopy. (a) Epilayer thickness (blue squares, left axis) and free carrier concentration (red circles, right axis) as a function of group V/III precursor ratio. (b) Epilayer thickness (blue squares, left axis) and (red circles, right axis) as a function of group V/III precursor ratio.

The dependence of LO phonon frequency (left axis) and free carrier concentration n_e(right axis) on V/III ratio are depicted in Fig. 5a, showing a decrease of n_e from 4.2×10^{19} to 1.7×10^{18} cm^{-3} and a shift of the LO-phonon frequency from 567 cm^{-1} as the group V/III precursor ratio varies from 900 to 2400.

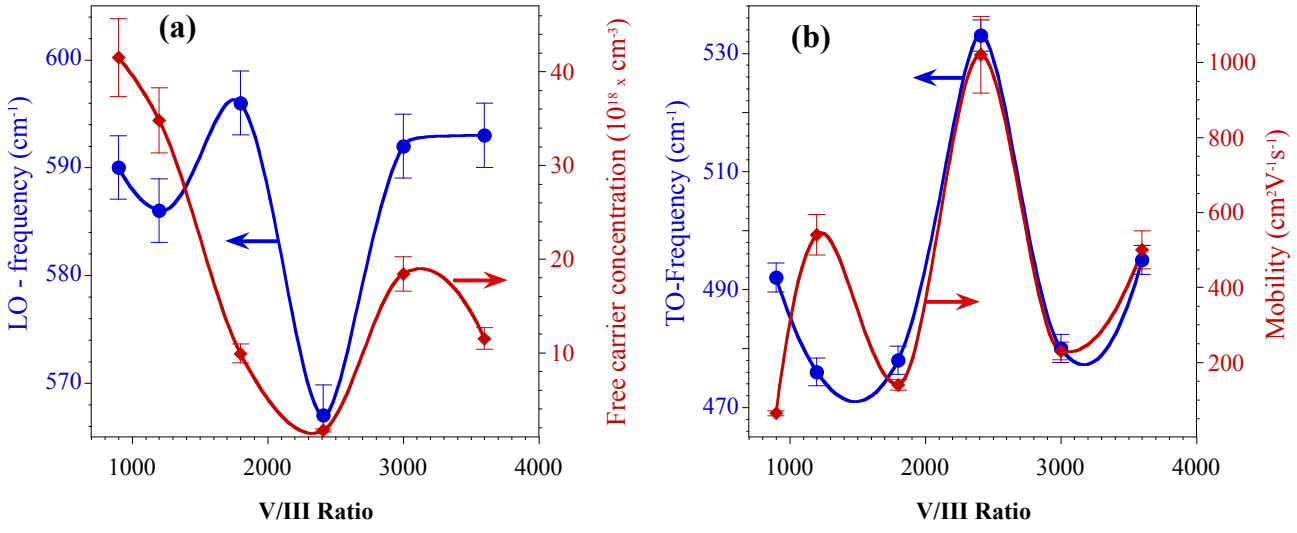

Figure 5. Group V/III molar precursor ratio dependence of the IR reflection. (a) ω_{LO} frequency (blue squares, left axis) and free carrier concentration (red circles, right axis) as a function of group V/III precursor ratio. (b) ω_{TO} frequency (blue squares, left axis) and mobility (red circles, right axis) as a function of group V/III precursor ratio.

As the group V/III ratio is further increased from 2400 to 3600, carrier concentration increases and the LO phonon frequency shifts towards higher frequencies. Figure 5b shows the dependency of TOphonon frequency (left axis) and free carrier mobility (right axis) as a function of the group V/III precursor ratio. With increasing V/III ratio from 900 to 2400, the carrier mobility μ increases from 64 to 1020 $cm^2V^{-1}s^{-1}$ and TO-phonon frequency shifts from 476 to 533 cm^{-1}. Both the carrier mobility and TO phonon frequency show a similar trend with V/III ratio. Khan *et al*.[26] have reported that the same behavior for the free carrier concentration and mobility for the bulk InN layer grown on AlN/sapphire templates. It is worthwhile to note in this study that the LO-phonon has a similar tendency as the free carrier concentration and shift of the TO-phonon has the same tendency with carrier mobility. The observed changes in the physical properties of the InN epilayers as a function of the V/III precursor ratio are summarized in Table 2.

Table 2. Summary of the optoelectronic properties obtained from FTIR data analysis and multi-layer stack model simulation, providing values for film thickness, growth rate, ω_{LO}, ω_{TO}, and free carrier concentration of the InN epilayers.

V/III Ratio	Thickness (nm)	Growth rate (nm/min)	Mobility ($cm^2V^{-1}s^{-1}$)	ω_{LO} (cm^{-1})	ω_{TO} (cm^{-1})	N_e (cm^{-3})
900	98	0.54	64	590	492	4.2×10^{19}
1200	111	0.62	540	586	476	3.5×10^{19}
1800	300	1.67	140	596	478	1.0×10^{19}
2411	360	2.00	1020	567	533	1.7×10^{18}
3000	324	1.80	230	593	495	1.8×10^{19}
3600	333	1.85	500	592	480	1.2×10^{19}

4. CONCLUSIONS

In summary, the effect of group V/III molar precursor ratio on the structural and optoelectronic properties of the InN epilayers have been investigated by XRD, Raman, and FTIR spectroscopies. The results show that the structural and optical properties of the InN epilayers vary strongly with different group V/III precursor ratio. An optimum in the structural properties is observed for a group V/III precursor ratio of 2400, where the Raman E_2(high) and XRD (0002) Bragg reflex exhibited lowest FWHM values of 7.53 cm^{-1} and 210 arcsec, respectively, with estimated grain size of 95 nm and an in-plane strain component of 3.8×10^{-4}. The calculated epilayer thickness for this V/III ratio was 360 nm (i.e. growth rate of 120 nm/hr), with a free carrier concentration of 1.7×10^{18} cm^{-3} and a carrier mobility of 1020 $cm^2V^{-1}s^{-1}$. Furthermore, the optical analysis indicate that with varying group V/III precursor ratio, the non-polar phonon mode of E_2(high) peak position remains constant; whereas, the polar phonon branches of transverse optical (TO) and longitudinal optical (LO) phonons are significantly shifted. The epilayer thickness increases the carrier mobility and reduces the free carrier concentration with increasing group V/III ratio. The analysis also revealed that free carrier concentration correlates with LO-phonon frequency; while, the carrier mobility follows the tendency of the TO-phonon frequency with group V/III ratio. The effect of group V/III molar precursor ratio on the surface morphology of the epilayers is presently under investigation.

5. AKNOWLEDGEMENT

This work was supported by the AFOSR grant # FA 9550-10-1-0097 and GSU-RPE. R. Atalay gratefully acknowledges the fellowship support from the Center for Diagnostic and Therapeutic at GSU.

REFERENCES

[1] Nanishi, Y., Saito, Y., and Yamaguchi, T., "RF-Molecular Beam Epitaxy Growth and Properties of InN and Related Alloys," Jpn. J. Appl. Phys. **42**, 2549 (2003).

[2] Higashiwaki, M., and Matsui, T., "Epitaxial growth of high-quality InN films on sapphire substrates by plasma-assisted molecular-beam epitaxy," J. Cryst. Growth **252**, 128-135 (2003).
[3] Davydov, V. Yu., Klochikin, A. A., Seisyan, R. P., Emtsev, V. V., Ivanov, S. V., Bechstedt, F., Furthmuller, J., Harima, H., Mudryi, A. V., Aderhold, J., Semchinova, O., and Graul, J., "Absorption and Emission of Hexagonal InN. Evidence of Narrow Fundamental Band Gap," Phys. Status Solidi B **229**, R1-R3 (2002).
[4] Wu, J., Walukiewicz, W., Yu, K. M., Ager III, K. M., Haller, E. E., Lu, H., and Schaff, W. J., "Narrow bandgap group III-nitride alloys," Phys. Status Solidi B **240**, 412-416 (2003).
[5] Nakamura, S., Senoh, M., and Mukai, T., "P-GaN/N-InGaN/N-GaN Double-Heterostructure Blue-Light-Emitting Diodes," Jpn. J. Appl. Phys. **32**, L8-L11 (1993).
[6] Meziani, Y. M., Maleyre, B., Sadowski, M. L., Ruffenach, S., Briot, O., and Knap, W., "Terahertz investigation of high quality indium nitride epitaxial layers," Phys. Status Solidi A **202**, 590-592 (2005).
[7] Lu, H., Schaff, W. J., and Eastman, L. F., "Surface chemical modification of InN for sensor applications," J Appl. Phys. **96**, 3577 (2004).
[8] Yamamoto, A., Islam, Md. R., Kang, T. T., and Hashimoto, A., "Recent advances in InN-based solar cells: status and challenges in InGaN and InAlN solar cells," Phys. Status Solidi C **7**, 1309-1316 (2010).
[9] Pollak, F. H., [Effect of Homogeneous Strain on the Electronic and Vibrational Levels in Semiconductors in Semiconductors and Semimetals], Vol. 32, ed. by Pearsall, T. P., Academic, New York, (1990).
[10] Nanishi, Y., Saito, Y., Yamaguchi, T., Araki, T., Miyajima, T., Naoi, H., "Recent development of InN RF-MBE growth and its structural and property characterization," Phys. Status Solidi C **1**, 1487-1495 (2004).
[11] Yamamoto, A., Adachi, M., and Hashimoto, A., "Enhanced two-dimensional growth of MOVPE InN films on sapphire (0001) substrates," J. Cryst. Growth **230**, 351-356 (2001).
[12] Hacker, V., and Kordesch, K., [Handbook of Fuel Cells-Fundamentals, Technology, and Applications], ed. by Vielstich, W., Lamm, A., and Gasteiger., H. A., John Willey & Sons, Inc. Chichester, England, (2003).
[13] Johnson, M. C., Konsek, S. L., Zettl, A., and Bourret-Courchesne, E. D., "Nucleation and growth of InN thin films using conventional and pulsed MOVPE," J. Cryst. Growth **272**, 400-406 (2004).
[14] Woods, V. T., and Dietz, N., "InN growth by high-pressure chemical vapor deposition: Real-time optical growth growth characterization," Mater. Sci. & Eng. B **127**, 239-250 (2006).
[15] Dietz, N., [III-Nitrides Semiconductor Materials - Indium-nitride growth by HPCVD: Real-time and ex-situ characterization], ed. by Feng, Z. C., Imprerial College Press, (2006).
[16] Dietz, N., Alevli, M., Atalay, R., Durkaya, G., Collazo, R., Tweedie, J., Mita, S., and Sitar, Z., "Optical Characterization of InN Layers Grown by High-Pressure Chemical Vapor Deposition," Appl. Phys. Lett. **92**, 041911-041913 (2008).
[17] Hu, Z. G., Strassburg, M., Dietz, N., Perara, A. G. U., Asghar, A., and Ferguson, I. T., "Composition dependence of the infrared dielectric functions in Si-doped hexagonal $Al_xGa_{1-x}N$ films on c-plane sapphire substrate," Phys. Rev. B **72**, 245326-245335 (2005).
[18] Langford, J. I. and Wilson, A. J. C., "Scherrer after sixty years: A survey and some new results in the determination of crystalline size," J. Appl. Cryst. **11**, 102-113 (1978).
[19] Davydov, V. Yu., Emtsev, V. V., Goncharuk, I. N., Smirnov, A. N., Petrikov, V. D., Mamutin, V. V., Vekshin, V. A., Ivanov, S. V., Smirnov, M. B., and Inushima, T., "Experimental and theoretical studies of phonons in hexagonal InN," Appl. Phys. Lett. **75**, 3297-3299 (1999).
[20] Janotti, A., Zhang, S. B., Wei, Su-H., and Van de Walle, C. G., N, "Effect of N on the electronic structures of H defects in III-V semiconductors," Optical Materials **25**, 261-269 (2004).
[21] Thakur, J. S., Haddad, D., Naik, V. M., Naik, R., Auner, G. W., Lu, H., and Schaff, W. J., "A_1(LO) phonon structure in degenerate InN semiconductor films," Phys. Rev. B **71**, 115203-115212 (2005).
[22] Thakur, J. S., Auner, G. W., Haddad, D., Naik, R., Naik, V. M., "Disorder effects on infrared reflection spectra of InN films," J. Appl. Phys. **95**, 4795-4801 (2004).
[23] Domenech-Amador, N., Cusco, R., and Artus, L., "Raman scattering study of anharmonic phonon decay in InN," Phys. Rev. B **83**, 245203 (2011).
[24] Holtz, M. E., Gherasoiu, I., Kuryatkov, V., Nikishin, S. A., Bernussi, A. A., and Holtz, M. W., "Influence of phonons on the temperature dependence of photoluminescence in InN with low carrier concentration," J. Appl. Phys. **105**, 063702-063705 (2004).
[25] Khan, N., Sedhain, A., Li, J., Lin, J. Y., and Jiang, H. X., "High mobility InN epilayers grown on AlN epilayers templates," Appl. Phys. Lett. **92**, 172101-172103 (2008).